The effect of growth parameters and mechanism of titania nanotubes prepared by anodic process

S. W. NG[*], F. K. YAM, K. P. BEH, S. S. TNEH, Z. HASSAN
School of Physics, Universiti Sains Malaysia, 11800 Penang, Malaysia

In this work, the physical characteristics of TiO_2 nanotubes grown under various anodizing parameters (composition of electrolyte, voltage, and anodizing duration) were investigated. The surface morphology and tube structure of the as-anodized TiO_2 nanotubes were characterized by SEM and TEM. Results showed that optimal growth can be obtained at 40 V, 0.6 wt% of fluoride and duration of 30 minutes. Based on the current transient profile obtained from anodization of Ti foil, a possible mechanism of the growth of TiO_2 nanotubes was proposed.

1. Introduction

Titanium dioxide (TiO_2), although having an indirect bandgap (~3.0 eV), gained much attention owing to its photocatalytic ability which enables the conversion of solar energy to electrical energy through the fabrication of dye-sensitized solar cells (DSSCs) [1-3]. However, the photocatalytic ability of TiO_2 depends heavily on its certain crystal structure. There are three well known crystal structures of TiO_2, namely anatase, rutile, and brookite. Among these crystal structures, anatase crystal exhibits superior photocatalytic ability [4], hence it is widely studied.

Nanostructured materials often allow more sensitive devices to be made, due to their large surface-to-volume ratio [3]. Various methods have been employed to fabricate such nanostructures. In TiO_2 case, well known nanostructures such as nanotubes, nanowires, nanosheets have been identified [3-7]. Methods such as anodization, template assisted method, and sol-gel [3,8,9] are the main attractions in making these structures.

Among these methods, anodization of titanium provides a faster way to obtain nanostructures [3]. Nanotubes are the typical nanostructures obtained using this method. In addition, anodization provides an extensive flexibility in terms of adjusting the physical properties of the nanotubes. By changing the anodizing environments, nanotubes with various sizes, aspect ratio can be obtained easily [2,3,5,9].

In present work, we demonstrate a series of TiO_2 anodizing environments in order to investigate the influence of various anodizing parameters on the nanotube growth. It is crucial to understand the nanotube formation mechanism so as to effectively manipulate the anodizing conditions and consequently obtain the desired nanotube structures. Apart from that, we propose a growth model to develop a better understanding of the formation of TiO_2 nanotube.

2. Experimental

High purity titanium sheet (Ti, 99.7%, Strem Chemicals, with thickness of 0.127 mm) was precut into 30 mm × 10 mm. Prior to anodization, Ti foils were mechanically polished under running water by Silicon Carbide (SiC) abrasives of 1200 grit, followed by 1500 grit; finally 2000 grit to obtain a flat and smooth surface. Ti foils were degreased by sonicating in acetone and ethanol for 5 minutes each, subsequently rinsed in deionized (DI) water and then dried under nitrogen stream.

The Ti foils were anodized using a conventional two-electrode configuration with Platinum (Pt) wire serving as a counter electrode. In consideration of exploring the influence of anodizing parameters towards the growth of nanotubes, a series of experiments with different parameters were carried out and the results were studied. The anodization condition of each sample is summarized in Table 1.

Table 1. Anodization conditions of Ti samples.

Sample	Electrolyte ratio			Concentration of NH$_4$F (wt%)	Applied Voltage (V)	Anodizing Duration (mins)
	DI water	Organic additives				
		EG	Glycerol			
A1	19	1	-	0.3	20	60
A2	19	1	-	0.6	20	60
B1	1	-	1	0.3	40	60
B2	1	-	1	0.6	40	60
C1	1	-	1	0.3	40	30
C2	1	-	1	0.6	40	30

EG: Ethylene Glycol

The anodization setup is shown in Fig. 1:
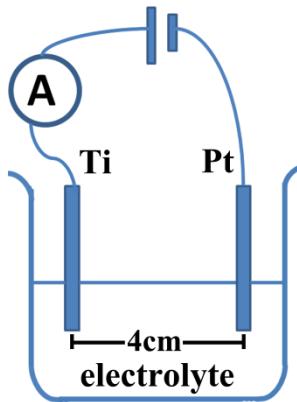
Fig. 1. Experimental Setup.

In the overall anodic process, the temperature of the electrolyte was kept constant at room temperature ambient. All electrolytes were stirred at a constant speed using a magnetic stirrer. In addition, the distance between the Ti foil and Pt wire was maintained at 4 cm apart. The current-transient profile of the anodization process was obtained by collecting data at elevated time steps.

The surface morphology of the samples was characterized using scanning electron microscopy (SEM) while elemental analysis of samples surface was done by energy dispersive x-ray spectroscopy (EDX). Prior to characterization, a thin layer of Pt film was sputtered on the surface of the samples to reduce charging effects caused by the semi-insulating TiO$_2$. The hollow nature of the nanotubes was determined using energy-filter transmission electron microscopy (EF-TEM).

3. Results and discussion

Based on our previous work on synthesizing TiO$_2$ nanotubes [10], we found that the grown nanotubes can be divided into two categories quantitatively. By referring to the surface of the nanotubes, if perfectly formed circular rims were present, we defined them as well-grown nanotubes; if the rims were irregularly shaped, we defined them as deformed nanotubes. Our current investigation here involved the influences of several anodizing parameters, namely fluoride concentration, voltage, and duration on the growth of TiO$_2$ nanotubes.

3.1 Structural characterization of nanotubes
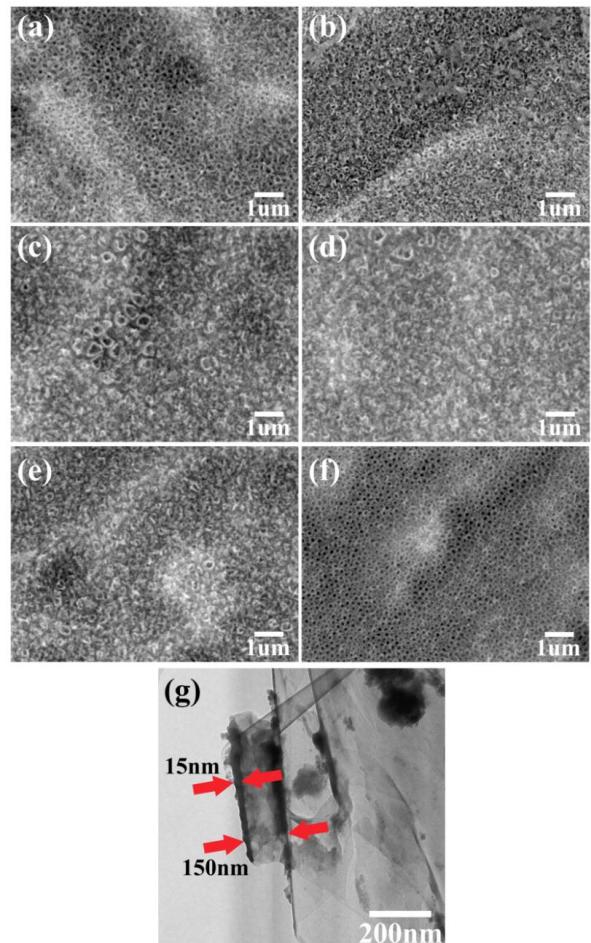
Fig. 2. SEM images with 10k magnification, top view of TiO$_2$ nanotube samples (a) A1, (b) A2, (c) B1, (d) B2, (e) C1, (f) C2 formed under different environment and (g) EF-TEM images of C2.

Fig. 2 shows the micrographs of the samples anodized under different conditions. In order to investigate the influence of fluoride concentration, we refer sample A1 and A2 for comparison. Both samples exhibited tube-like structure. It can be noted that well-grown nanotubes can be obtained if the fluoride concentration used was lower. At higher concentration, deformed nanotubes were observed. This suggested that the nanotubes were prone towards etching process by fluoride ions.

Comparing samples A1 and B1 will lead to the effects of anodizing voltage towards nanotubes growth. It is discernable that nanotubes formed under higher potential having larger pores. Another notable feature when comparing these two samples is the order of the nanotubes. When Ti foil was anodized under lower potential, highly ordered and closely packed nanotubes were observed. A large gap between nanotubes has been seen in sample B1. One plausible explanation would be the gaps formed between nanotubes were due to dielectric breakdown of the oxide layer.

The time taken for the anodizing process was nevertheless an important parameter to be considered. Comparing samples B2 and C2, it is clearly shown that Ti foil anodized at a shorter duration yield well-grown nanotubes. This is because at longer duration, dissolution of the nanotubes was more likely to occur.

Among the grown nanotubes, sample C2 yield highly ordered and closely packed nanotubes. Due to its condition, it might contradict the earlier points stated. However, anodizing parameters are always mutually dependent on each other. Hence, the physical characteristics of the nanotubes might differ from each other. Furthermore, during the earlier discussions, samples were compared pair-by-pairs, thus, the aforementioned facts do not contradict each other.

An EF-TEM image of sample C2 in Fig. 2(g) was included to verify the hollow nature of the nanostructure. The nanotube diameter is apparently greater than 100 nm with wall thickness approximately 15 nm. Due to sample preparation for EF-TEM characterization, which involved detaching the nanotubes from Ti foil by means of sonicating, shattered nanotubes were obtained. Thus it is unable to report the actual tube length from TEM image.

To examine the composition of TiO_2 nanotubes, elemental qualitative analysis was employed at random surface area consisting of compact nanotubes array. A representative EDX spectrum which shows the elements present on the surface of TiO_2 nanotubes is shown in Fig. 3. Only EDX spectrum of sample C2 is shown since all samples exhibit a similar spectrum.
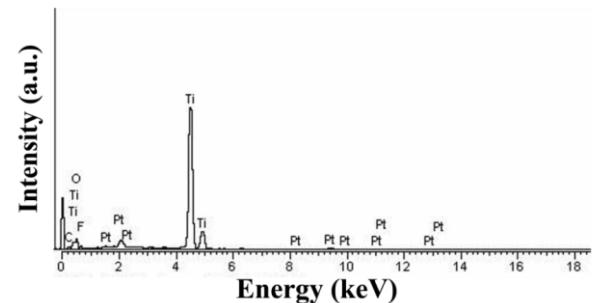
Fig. 3. EDX spectrum of sample C2.

Two dominant components in TiO_2 nanotubes are Ti and O as these peaks were discernable in Fig. 3. In addition, there was evidence of F and C peaks. The presence of F element is due to the usage of NH_4F while C element from organic additives which were essential components in the formation of nanotubes. The tiny Pt peaks were due to the coating layer on the sample prior to SEM and EDX characterization. The purpose of coating an ultrathin Pt layer is to prevent accumulation of static electric charges at surface of sample thus obtain sharper SEM images.

3.2 Mechanism of nanotube formation

By comparing the current transient profile of sample A1 and C1, in which their electrolyte ratio, aqueous-to-organic additives was 19:1 and 1:1 respectively, both profiles appeared in a similar trend as shown in Fig. 4.

Fig. 4. Current transient profile for sample (a) A1 and (b) B1. Insets are magnification of current from 50s to 750s.

At the beginning of each anodic process when potential was applied to the system, Ti^{4+} cations were discharged from Ti metal foil. Concurrently, O^{2-} and some
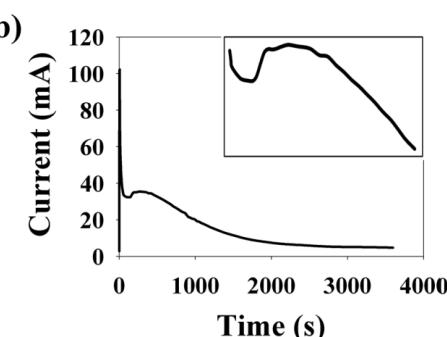
OH^- anions from the electrolyte drifted towards the anode. Hence current hiked to a sharp peak within first 15seconds

was observed. The chemical reaction happened at anode and cathode is given as below

$$Ti \rightarrow Ti^{4+} + 4e^- \qquad 2H^+ + 2e^- \rightarrow H_2 \qquad (1)$$

Within the next 30 seconds a thin and compact oxide layer was formed on the exposed titanium surface. Current fell drastically because the oxide layer acted as a barrier to resist the attack of anions on the surface of Ti. The formation of oxide layer can be described in Eq. (2) and (3). [2,3,8]

$$Ti^{2+} + 2H_2O \rightarrow TiO_2 + 4H^+ \qquad (2)$$

$$Ti + 2O^{2-} \rightarrow TiO_2 + 4e^- \qquad (3)$$
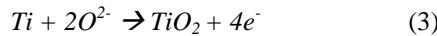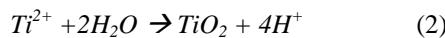
The initial formation of thin pits and cracks on the oxide surface caused a redistribution of charges. The charges produced a local electric field which provided a field-assistance to the dissolution of oxide layer for the erosion of pits. These tiny pits eventually evolved into tubular structure. This was shown by a slight increase of current B1 and the current remained constant for a short interval. [6,8,9]

The migration of O^{2-} anions was random and covered the entire surface, hence array of TiO_2 nanotubes were randomly formed over the Ti surface. The nanotube formation process is a competition between oxide layer dissolution and nanotube formation. It can be described in Eq. (5). [2,3,8]

From Eq. (2) and (3),

$$Ti + 2H_2O \rightarrow TiO_2 + 4H^+ + 4e^- \qquad (4)$$

$$TiO_2 + 4H^+ + 6F^- \leftrightarrow [TiF_6]^{2-} + 2H_2O \qquad (5)$$
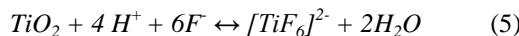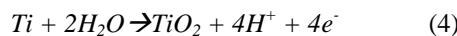
And from Eq. (4) and (5), reaction between TiO_2 and fluoride (F^-) anions formed soluble $[TiF_6]^{2-}$ complex ions.

After a period of time, the nanotube formation rate is higher than that of oxide layer dissolution rate. The higher formation rate yielded elongation of TiO_2 nanotubes. However, the migration rate of anions decreased as the thickness of oxide layer increased with time. Therefore, current of A1 and B1 decreased slowly until both currents reached a steady state at 1800 seconds. A noteworthy difference between the current of these to samples is that the former decreased with small fluctuation while current decrement of the latter was smoother as shown in insets of Fig. 4. This again, demonstrated the influence of viscosity of organic electrolyte to the nanotube formation [1] where current fluctuation is less significant in organic additives electrolyte of higher concentrations, i.e. set B.

Thereafter, the growth of nanotubes continued until a point where the dissolution rate is equal to the formation rate. An equilibrium state was achieved and both currents remained almost constant until the end of each anodic process at 3600 seconds.

Current transient of R9S1 exhibited identical characteristics as current of B1. It is commonly reported that a longer tube length can be obtained by prolonging the anodic process [1]. However take note that anodization duration of set B was twice of set C and recall Fig. 2 (c) – (f), the surface morphology of nanotubes of set B is generally less favourable than that of set C. This is because tube walls started to deform when dissolution of oxide layer increased slowly with the increase of time. It is derived that there is a compromise between tube length and uniformity of tube surface or tube wall. On top of that, it is observed that Eq. (5) is a reversible process. A desirable tube conditions could be attained by controlling the reaction between TiO_2 and $[TiF_6]^{2-}$ ions.

For better understanding of nanotube formation mechanism, a possible growth model is proposed as below.
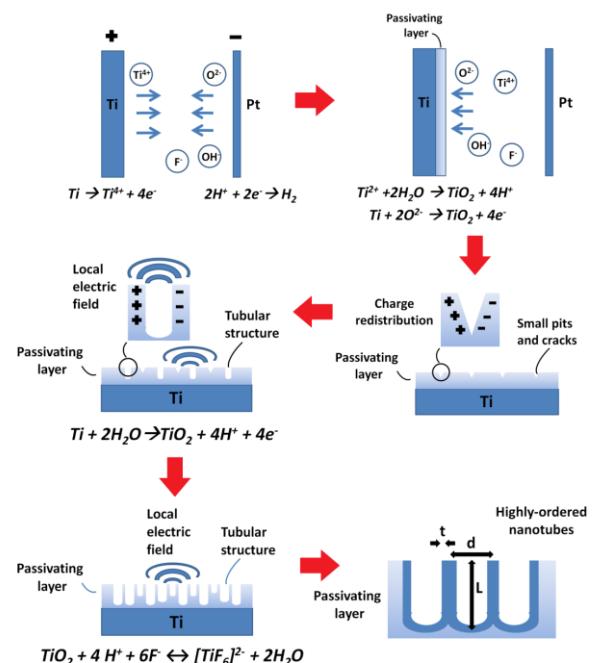
t: wall thickness, d: tube diameter, L: tube length

Fig. 5. Schematic growth model of formation of highly-ordered TiO_2 nanotubes.

4. Conclusion

TiO_2 nanotubes were successfully fabricated by anodic process of different anodizing environment. The effects of anodizing environment on morphology and structural properties of TiO2 nanotubes have been studied. TiO_2 nanotubes obtained under optimal condition in current work were of diameter 100nm and wall thickness of 15 nm. Through the study of nanotube formation mechanism, it is discovered that the nanotube formation process is a competition between oxide layer dissolution and nanotube formation. Also, tube structure can be modified by altering the reaction between oxide TiO_2 and complex ion $[TiF_6]^{2-}$.

Acknowledgements

References

[1] J. M. Macak, P. Schmuki, Electrochim. Acta **52**, 1258 (2006).

[2] J. M. Macak, H. Hildebrand, U. Marten-Jahns, P. Schmuki, J. Electroanal. Chem. **621**, 254 (2008).

[3] Xiaofeng Yu, Yongxiang Li, Wojtek Wlodarski, Sasikaran Kandasamyc, Kourosh Kalantar-zadeh, Sensor. Actuat. B-Chem **130**, 25 (2008).

[4] S. Sreekantan, R. Hazan, Z. Lockman, Thin Solid Films **518**, 16 (2009).

[5] Grzegorz D. Sulka, Joanna Kapusta-Kołodziej, Agnieszka Brzozka, Marian Jaskuł, Electrochim. Acta **55**, 4359 (2010).

[6] Xiaobo Chen, Maria Schriver, Timothy Suen, Samuel S. Mao, Sensor. Actuat. B-Chem **130**, 25 (2008).

[7] C. L. Chok, B. L. Ng, F. K. Yam, J. Optoelectron. Adv. Mater. **4**, 148 (2010).

[8] Ruixia Ge et al. Mater. Lett. **62**, 2688 (2008).

[9] Soon Hyung Kang, Jae-Yup Kim, Hyun Sik Kim, Yung-Eun Sung, J. Ind. Eng. Chem. **14**, 52 (2008).

[10] F. K. Yam, K. P. Beh, S. W. Ng, Z. Hassan ,Thin Solid Film (2010) (submitted for publication).

_____
*Corresponding author: sw.ng@live.com, yamfk@usm.my